14th Australasian Fluid Mechanics Conference
Adelaide University, Adelaide, Australia
10-14 December 2001

The Effect of Turbulence Intensity on Stall of the NACA 0021 Aerofoil

K. E. Swalwell, J. Sheridan and W. H. Melbourne

Department of Mechanical Engineering

Monash University, Clayton, Victoria, 3800 AUSTRALIA

Abstract

This paper presents lift and drag data obtained from pressure taps on a NACA 0021 aerofoil at Reynolds numbers of around 3.5 x 10^5 over a wide range of angles of attack. The airfoil was subjected to low turbulence flow of turbulence intensity 0.6%, and turbulent flows of length scale 0.56 chords and intensities of 4% and 7%. Turbulence was found to delay stall in a way that is consistent with the delayed stall seen on Horizontal Axis Wind Turbines. Increasing the turbulence intensity delayed stall until higher angles of attack. Further work is proposed to investigate the reasons for this delay, to repeat this experiment on a thick cambered aerofoil and to assess the likely effect on wind turbine performance.

Introduction

Predicting the aerodynamic performance of wind turbines is important in evaluating the expected power production of different designs. It also determines the strength and fatigue resistance that turbine components require to survive over their design lifetime. To predict the aerodynamic performance of Horizontal Axis Wind Turbines (HAWTs) the Blade Element Momentum (BEM) method is commonly used. This method equates the performance of a small section of the wind turbine blade to the performance of an aerofoil section of the same profile in the wind tunnel. Using the aerofoil's lift and drag coefficient (C_L and C_D respectively) curves an iterative process is used to deduce an equivalent angle of attack (α) from the wind speed (V) and rotational speed of a blade element (for a complete explanation of the BEM method see [3]). As the wind speed increases the angle of attack increases. A predicted performance curve derived using the BEM method is shown in Figure 1.

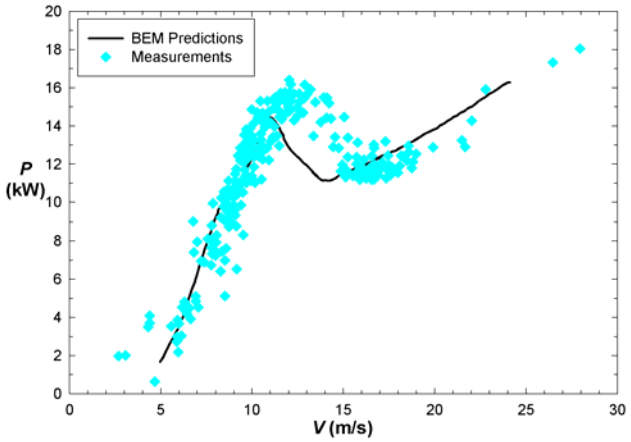

Figure 1. Comparison of the power output (P) predicted by the BEM method and the measured performance in the field at different wind speeds (V) [8]. NREL obtained each data point by selectively averaging data during periods of steady wind and minimal yaw. The averaged data represents less than 1% of the total measurements.

The BEM method predicts performance well when wind turbines are operating at angles of attack below those at which the aerofoil sections stall in the wind tunnel and at small yaw angles. Van Grol, Snel & Schepers (as quoted in [4]) reported that the BEM method predicts power and annual energy yield to an accuracy of ±8% for such conditions. However, the BEM method consistently underpredicts the turbine's performance at wind speeds corresponding to angles of attack above stall on the aerofoil section in the wind tunnel. This under prediction is seen in Figure 1. Even turbines that pitch the blades to avoid stall do not avoid this extra load, as the pitching mechanisms are too slow to avoid stall conditions during wind gusts.

Several theories have been advanced to explain what is commonly called delayed stall. One that has not been looked at in depth from an aeronautical perspective, although it is known to be important from a structural viewpoint, is turbulence. It should be emphasised that delayed stall has been seen in situations of low turbulence, such as that shown in Figure 1 and Ebert and Wood's [2] wind tunnel tests of a small wind turbine, so it is clearly not the only important factor in delayed stall.

Much work has been done on the effect of turbulence intensity and scale on bluff bodies. Turbulence is known to interact with boundary layers promoting their transition from laminar to turbulent. In free shear layers separating from the leading edge added turbulence causes a higher radius of curvature of the shear layer and therefore earlier reattachement [6]. In cylinders it is known that for all three transition states if the turbulence length scale is less than the diameter and intensity is greater than a certain value that turbulence becomes a governing factor [11].

Surprisingly little work has been done on the effect of turbulence on the performance of aerofoils. The first major study was conducted by Stack in 1931 [9]. He measured the lift and drag characteristics of several aerofoil sections of 5 inch chord (c) and 30 inch span with and without a turbulence generating grid in the flow. For the NACA 0021 aerofoil section he found that turbulence increased the maximum C_L and delayed stall for Reynolds numbers based on chord (Re) above 1 x 10^5. Unfortunately the scale and intensity of turbulence produced by the grid was not measured. Stack's results for the NACA 0021 aerofoil are shown in Figure 2.

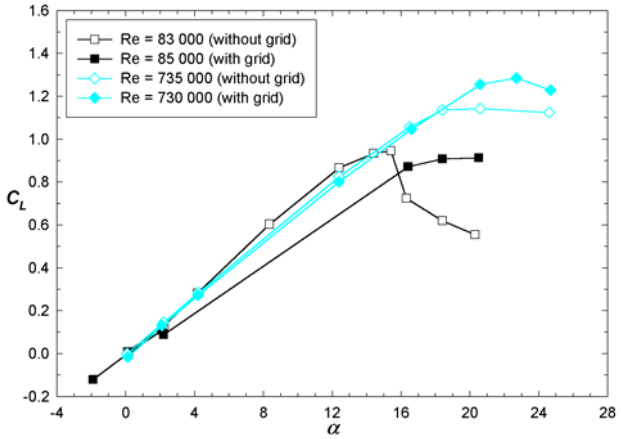

Figure 2. The effect of turbulence on the performance of a NACA 0021 aerofoil section [9].

Figure 2 shows for a *Re* of 83 000 without a grid the aerofoil stalls abruptly at an α of about 16°. For a similar *Re* with turbulence the lift is still increasing at α beyond 16°. No data points were taken between α of 4° and 16° for this case so where the results deviate from the low turbulence case is unclear. A similar delay in stall is observed between measurements for a *Re* of 735 000 without a grid and a *Re* of 730 000 with a grid. Stall in the low turbulence flow at a *Re* of 735 000 is less abrupt than at a *Re* of 83 000.

Thick cambered aerofoils are usually used at the root of wind turbine blades, the part of the blade that stalls first. However, for the two thick cambered aerofoils he tested, Stack found that adding turbulence decreased the maximum C_L. For the USA 35A aerofoil the decrease was observed over a *Re* range of 1.7 x 10^5 to 2 x 10^6. If this is true of all thick cambered aerofoils the effect of turbulence on lift could not be contributing significantly to delayed stall on HAWTs. Stack also found a similar reduction in the maximum C_L on the NACA 0006 section. This occurred when turbulence was added to the flow for a *Re* range of 1.8 x 10^5 to 1.8 x 10^6. Jancauskas [5], as part of his study of the effect of turbulence on bridge like structures, also looked at the effect of turbulence on a NACA 0006 section. This section had an aspect ratio 2.67. His findings contradict those of Stack. Jancauskas found that turbulence delayed stall on the NACA 0006 aerofoil at a *Re* of 2 x 10^5. He also found that as the turbulence intensity was increased from 0.6 % to 16 % stall was further delayed.

The other major interest in the effect of turbulence on the performance of aerofoils is in the field of aeroacoustics. Mish & Devenport [7] investigated the effect of two different scales of turbulence of similar intensity to compare with predicted aeroacoustic performance on a NACA 0015 aerofoil of aspect ratio of 3. The two length scales were 0.134*c* and 0.0127*c* at intensities of 3.93% and 4.35% respectively. Both levels of turbulence delayed stall but the longer length scale caused less effect than the shorter length scale.

Because of the difference in results between Stack and Jancauskas for the NACA 0006 aerofoil it was decided to investigate the validity of Stack's results for cambered thick aerofoils. As a first stage in this process the NACA 0021 aerofoil was tested to obtain data for comparison with the thick cambered NACA 4421 aerofoil, which has been used on some wind turbines. This paper presents the results of this first stage. Due to Jancauskas' results showing the importance of turbulence intensity two different turbulence intensities were tested. The turbulence length scale was chosen to be less than the chord length.

Experimental Method

A smooth NACA 0021 aerofoil section with a chord length (*c*) of 125 mm was used for this experiment. The aerofoil was constructed of carbon fibre and had two internal steel bars running its length for strength and stiffness. The aerofoil had several rows of pressure taps, as shown in Figure 3. However only the average results from row B will be reported here.

The experiments were carried out in the 2 by 1 meter section of the 450 kW wind tunnel at Monash University. End plates were positioned to give an aspect ratio of 7.28. The high aspect ratio was chosen to avoid the suppression of cross flows by the end plates, as has been seen in experiments on cylinders. Szepessy & Bearman [10] tested a cylinder using end plates to give different aspect ratios with a Reynolds number range of 8 x 10^3 to 1.4 x 10^5. They found that aspect ratios above 7 were necessary to stop the end plates suppressing cross flows and therefore increasing the magnitude and decreasing the frequency of the fluctuating lift forces.

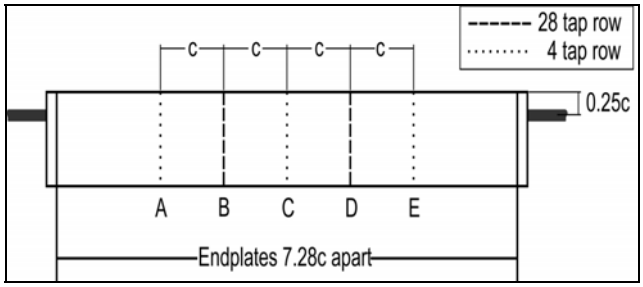

Figure 3. Tapping Row Positions.

The pressure taps in row B were positioned as shown in Figure 4. with a higher concentration of taps towards the leading edge. Each tap consists of a metal tube mounted flush with the surface and connected via a 1700 mm long PVC tube to a Scanivalve transducer. The transducers were set to measure the difference between the surface pressure and the tunnel static pressure. Samples were taken at 1000 Hz for 35 seconds to get the data at each α. These samples were averaged over the 35 second period to give an average pressure at each tap for each angle of attack. This was divided by the dynamic pressure measured by a Pitot tube in the tunnel connected to the Scanivalve to give the coefficients of pressure (C_P). The C_L and C_D curves were calculated using MATLAB. By fitting a spline to the measured C_P across the surface the C_L and C_D could be calculated on small sections of the aerofoil surface for each α. By adding the calculated values around the whole surface for each angle of attack the C_L and C_D curves versus α were created.

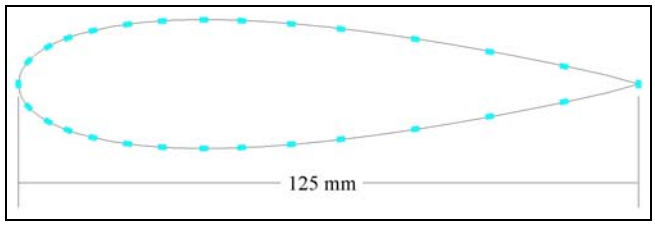

Figure 4. Aerofoil Tapping Positions Row B.

Turbulence was generated by a grid placed at different distances upstream of the model. The intensities and scales of the generated turbulence and the *Re* range of each test are given in Table 1. The Reynolds numbers that the tests were conducted at varied due to the extra loads on the fan caused by the turbulence grids. This was compensated for to a limited extent by increasing the fan blade angle for each test. During the tests *Re* varied due to the unstalled aerofoil slowing the flow and because of variations in tunnel temperature.

Grid Position	*Re* (x10^5)	I_u (%)	I_v (%)	I_w (%)	$\frac{L_{ux}}{c}$	$\frac{L_{uy}}{c}$	$\frac{L_{uz}}{c}$
No Grid	3.9 ±0.1	0.6	0.6	0.6	-	-	-
3.55 m	3.5 ±0.1	7	7	7	0.56	0.56	0.56
5.6 m	3.4 ±0.1	4	4	4	0.56	0.56	0.56

Table 1. Grid Positions and Resultant Turbulence Intensities and Length Scales. (Grid position is defined as the distance from the grid to the pivot point of the aerofoil at 0.25*c*). Measurements from [1].

Results and Discussion

Measurements of the pressure coefficients were taken at α in 2.5° increments from 0 to 35°, 5° increments from there to 70° and at 90°. The C_L and C_D calculated from these measurements are presented in Figure 5.

The lift curves show that the addition of turbulence delays stall. This is despite the higher *Re* values of the lower intensity tests, which would generally increase the C_L, as was shown by Stack's measurements. The low turbulence flow shows an abrupt cut off in lift, similar to that seen in Stack's low turbulence and low *Re* measurements but at a lower α. Higher *Re* values in the low turbulence may explain why this case generally shows a slightly higher C_L for angles of attack up to 10°. Drag in all cases is very similar until α is above 12.5°.

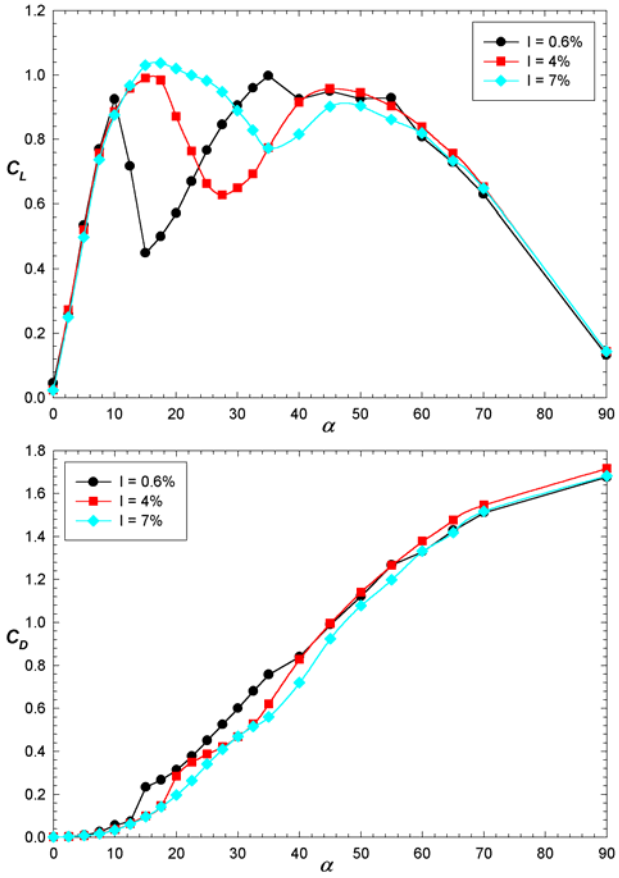

Figure 5. Lift and Drag Coefficients for each angle of attack.

At an α of 10° the lift curve in all cases has strayed slightly from the linear relationship with α, indicating that the stalling process has begun. The low turbulence case shows a sudden stall at an α above 10°. This is followed by a jump in the C_D at 12.5°. In contrast, the C_L for the 4% turbulence intensity doesn't begin to decrease until an α of about 17.5°, and even then decreases more slowly. This is also followed by a jump in C_D at an α of 20°. The decrease occurs even more slowly for the 7% turbulence intensity case. There is no discernable jump in C_D in this case.

Following the initial decrease in C_L associated with stall it increases again. This is characteristic of lift curves over a wide range of angles of attack and is due more to the general deflection of air downwards at these angles of attack rather than any attached flow. These are associated with fairly large C_D. It is interesting to note that the C_L for the low intensity case exceeds all the pre-stall values case at an α of about 30°. By an α of 40° the lift and drag curves for the 0.6% and 4% turbulence intensity match fairly well; by 60° this is also true for the 7% intensity curves.

Initially the drag curve at an α of 90° was expected to go to that of a flat plate at about 2 and the lift curve to go to zero. However, instead there was still positive lift at an α of 90°. This may have been due to the non-symmetrical shape presented to the flow at this α. The pressure measurements at an α of 90° (not shown) reveal that there is suction pressure on both sides of the rounded leading edge which would result in slight lift. This flow probably also causes the smaller drag.

Figure 6 shows the C_P around the aerofoil for the different cases to give more detail about what is occurring for different angles of attack. The zero α case is given as an indication of the accuracy of the measurements. Ideally all the points for the upper and lower surface for each case should lie on top of each other. The average pressure coefficients are slightly higher for a turbulence intensity of 0.6% than at 4%. These results, and the even lower C_P at 7%, are probably due to the higher *Re* number of these tests. The small spread in the pressure coefficients from the top and bottom surfaces of the aerofoil is probably due to a combination of slight errors in the angle of the aerofoil in the wind tunnel and small errors in the positioning of the pressure taps. This would be especially important on the leading edge where, because of the rapidly changing pressure gradient, small errors in placement could significantly influence the measured pressure coefficient.

At an angle of 10° all the pressure coefficients show attached flow, as would be expected. There is a small double humped variation in C_P on the suction surface. This is assumed to be evidence of a small separation and reattachment zone.

The double humped feature persists in the suction side for pressure coefficients taken in a 7% turbulence intensity flow up to an α of 20°. In these conditions the flow is clearly still attached at the leading edge, although it is unclear whether it has separated before it reaches the trailing edge. Some evidence for the double humped feature can also be seen in the 4% turbulence intensity case at this angle of attack but the suction pressure at the leading edge is lower than the 7% turbulence intensity case. In the 0.6% turbulence intensity flow the aerofoil was fully stalled at an α of 20° and there is no evidence for this double humped characteristic. Another difference between the three different intensity flows is the effect on the trailing edge pressure. The suction pressure on the trailing edge increases as turbulence intensity decreases.

By an α of 30° the aerofoil in the 4% turbulence intensity flow also appears fully stalled and the aerofoil in the 7% flow appears only to be attached on the leading edge. Interestingly, although both appear to be fully stalled, there is more suction on the top surface of the aerofoil in the 0.6% turbulence intensity flow than in the 4% turbulence intensity flow and the flow close to the trailing edge in the 7% turbulence intensity flow. This suction causes the C_L for the 0.6% and 7% turbulence intensity cases at an α of 30° to be very similar and higher than the C_L for the 4% turbulence intensity flow. This may be due to a wider wake in the low turbulence case and therefore higher suction pressure.

At an α of 30° it is also interesting to note that the trailing edge pressures for the 4 and 7% turbulence intensity flows are again equal while for the 0.6% intensity flow the suction pressure on the trailing edge is considerably higher. The wider wake in the low turbulence case could also be causing this.

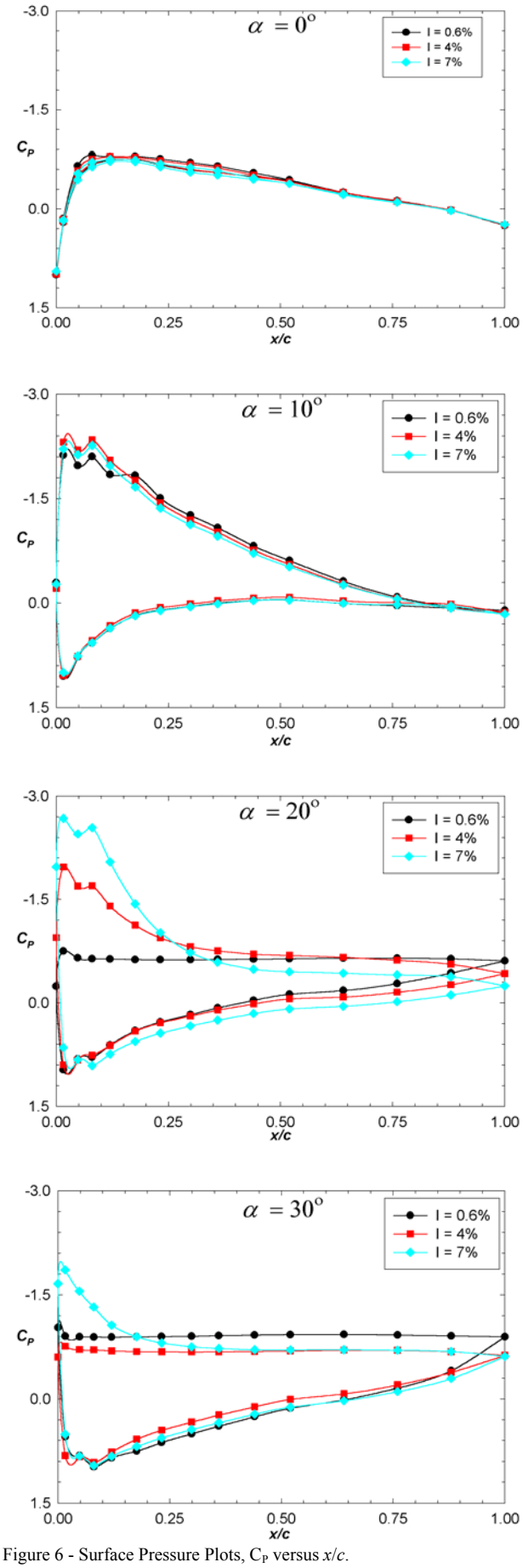

Figure 6 - Surface Pressure Plots, C_P versus x/c.

Further Work

Analysis of the instantaneous pressures is planned to examine more closely the higher C_L for the lowest turbulence intensity flow between 30 and 40° and the double humped characteristic found at some angles of attack near the leading edge on the suction side of the aerofoil. More testing at the same *Re* with different grids should shed more light on the whether these effects are dependent on turbulence intensity or *Re*.

However, this preliminary set of results are promising and bode well for the next set of tests to be conducted on a cambered version of this aerofoil, the NACA 4421. If these tests also show delayed stall the experiment may be repeated in the 1.5 MW tunnel at Monash to test the hypothesis at higher *Re* more appropriate to large scale wind turbines.

Conclusions

The addition of turbulence of a length scale of 0.56c and intensity of 4% was found to delay stall on the NACA 0021 model in accordance with previous results. Increasing the turbulence intensity to 7% delayed stall further.

Acknowledgments

Primary support for this research program was provided by a Monash Graduate Scholarship. The turbulence intensity and scale data was kindly provided by Mr. Michael Eaddy. Thanks must also go to SP Systems, Australia for kindly donating the carbon fibre and epoxy used to construct the aerofoil section and to the Department of Mechanical Engineering workshop staff, especially Mr. Don McMaster and Mr. John Hick, for their advice and the construction of the aerofoil section and supports.

References

[1] Eaddy, M., Melbourne, W. H. & Sheridan, J., "Effect of Surface Roughness and Free Stream Turbulence on the Axial Correlation Length of a Circular Cylinder", in *Proceedings of the 14th Australasian Fluid Mechanics Conference*. 2001. Adelaide University, Adelaide, Australia.

[2] Ebert, P. R. & Wood, D. H., "The Near Wake of a Model Horizontal-Axis Wind Turbine - I. Experimental Arrangements and Initial Results", *Renewable Energy*, **12** (3), 225-243, 1997.

[3] Eggleston, D. M. & Stoddard, F. S., *Wind Turbine Engineering Design*, Von Nostrand Reinhold, New York, 1987.

[4] Hansen, A. C. & Butterfield, C. P., "Aerodynamics of Horizontal-Axis Wind Turbines", *Annual Review of Fluid Mechanics*, **25**, 115-149, 1993.

[5] Jancauskas, E. D., *The Cross-Wind Excitation of Bluff Structures and the Incident Turbulence Mechanism*, PhD Thesis, Mechanical Engineering, Monash University: Clayton, 1983.

[6] Melbourne, W. H., "Turbulence and the Leading Edge Phenomenon", *Journal of Wind Engineering and Industrial Aerodynamics*, **49**, 45-64, 1993.

[7] Mish, P. F. & Devenport, W. J., "Mean Loading Effects on the Surface Pressure Fluctuations on an Airfoil in Turbulence", in *Proceedings of the 7th AIAA/CEAS Aeroacoustics Conference*. 2001. Maastricht, The Netherlands.

[8] Simms, D. A., Hand, M. M., Fingersh, L. J. & Jager, D. W., "Unsteady Aerodynamics Experiment Phases II-IV Test Configurations and Available Data Campaigns", National Renewable Energy Laboratory (NREL), Golden, Colorado, 1999.

[9] Stack, J., "Tests in the Variable Density Wind Tunnel to Investigate the Effects of Scale and Turbulence on Airfoil Characteristics", NACA Langley Memorial Aeronautical Laboratory, Langley Field, VA, United States, 1931.

[10] Szepessy, S. & Bearman, P. W., "Aspect Ratio and End Plate Effects on Vortex Shedding from a Circular Cylinder", *Journal of Fluid Mechanics*, **234**, 191-217, 1992.

[11] Zdravkovich, M. M., *Flow Around Circular Cylinders*, Oxford University Press, 1997.